# Quantum optics and electrodynamics in microstructures

S Dutta Gupta[1] and G S Agarwal[2]

## ABSTRACT

We review some of the exciting features of the whispering gallery modes of dielectric microspheres. We present recent results on the applications of these whispering gallery modes in quantum optics, especially in the area of cavity quantum electrodynamics.

1. School of Physics, University of Hyderabad, Hyderabad 500046
   Email: sdgsp@uohyd.ernet.in
2. Physical Research Labopratory, Navrangpura, Ahmedabad 380009
   Email: gsa@prl.ernet.in

## 1. Introduction

One of the central issues of quantum optics has been the precise control of the radiative properties of atoms. It is now well understood that a suitable modification of the environment can lead to renormalization of the basic characteristics of an atom, namely, its decay rate and the transition frequency [1,2]. All through this paper we will refer to the environment as the cavity (at least in a generalized sense). Over the past few decades there has been a tremendous growth of the research activities centered on the cavity induced modifications of the atomic characteristics, leading to the now vast topic of cavity quantum electrodynamics (QED) [3]. The interest in this area is motivated by several factors. The QED manipulation of the atom can lead to enhancements, for example, in the spontaneous rate and the nonlinearity parameters [4], leading to zero threshold nonlinear processes. In fact, zero threshold lasing has been reported using the QED enhancement in different kind of cavities [5,6]. Depending on whether the cavity is “good” or “bad” one can distinguish between two regimes of cavity QED. In a bad cavity, when the photon emitted by the excited atom is short lived, it escapes the cavity before it can interact back with the atom. This irreversible process leading to nominal modifications of the decay rate and a frequency shift can be treated in the framework of a perturbation theory and is referred to as the weak-coupling regime. On the contrary, in a good cavity a novel kind of physics can be expected since the photon being long lived, can reexcite the atom. This leads to a periodic exchange of energy between the atom and the photon. The periodic exchange results in a doublet in the spectrum due to the so-called vacuum field Rabi splittings [7-10].

It is thus clear that in order to achieve the strong interaction regime it is necessary to have a cavity with larger and larger quality factors. In the context of Fabry-Perot (FP) cavities this has been achieved by using better and better mirrors, in some cases replacing the mirrors by distributed feedback structures. Naturally all these achievements needed considerable technological efforts. In contrast, there are systems, which due to their morphology, support very high quality factor modes. A classic example is the whispering gallery modes (WGM) of dielectric microspheres [11]. Quality factors of the order $10^{10}$ in the visible domain are now regularly achieved. Note that the fabrication technology for such microspheres is comparatively simple [12]. The structures, and hence the modes are robust. In view of the large Q-factors and associated large local field enhancement of the WGM's almost all nonlinear phenomena including lasing and bistability have been observed [13-16]. We need to stress that most of these processes are characterized by very nominal threshold powers. Note also that unlike in FP cavities the WGM's are not equispaced, leading to the remarkable possibility of having lasing at several different frequencies. Another property of the WGM, which is quite attractive from the viewpoint of cavity QED, is their low mode volume. This is a direct consequence of the localization of the mode near the rim of sphere. This was noted by Agarwal etal [17] who first suggested the use of WGM's to probe the strong interaction regime of cavity QED. Earlier there have been several observations of WGM induced weak interaction effects both in liquid and solid systems [18,19].

The organization of the review is as follows. We start with a basic and then more in-depth introduction to the WGM's in Section 2. We also consider briefly the effects of minor deviations from sphericity. In Section 3 we discuss modern methods for exciting

and characterizing such modes. Section 4 deals with the scope of WGM's in the context of nonlinear optics and lasing. Section 5 discusses the weak interaction regime of cavity QED, while in Section 6 we present a model calculation for the strong interaction regime. In Section 7 we present a unified Green's dyadic based approach, which explains both the regimes in terms of the specifics of the Green's function. Finally in Section 8 we indicate some of the important current and future directions in WGM cavity QED. We concentrated mostly on WGM's while, whenever necessary, we cited the results for planar micro cavities. This was done in order to ensure a broader perspective dealing with the same physical principles.

## 2. Whispering gallery modes of microspheres

Imagine that a ray resident inside a microsphere of a radius $a$ and relative refractive index $\overline{m}$ hits the interface at an angle larger than the critical angle for total internal reflection. Obviously the ray will bounce off the surface after each act of total internal reflection, never escaping the sphere. This may result in a 'mode' of the sphere provided that the principal quantum number $n$ associated with this mode satisfies the inequality

$$x \le n \le \overline{m}x, \qquad (1)$$

where $x = 2\pi a/\lambda$ is the size parameter. The left (right) inequality in Eq.(1) represents the resonance condition just outside (inside) of the sphere: the optical path outside (inside) has to be integer multiples of wavelength $\lambda$. We assumed that the sphere is in vacuum. Many of such simple features of electromagnetic wave scattering by dielectric spheres can be understood based on the ray optics or eikonal approximation [21] especially for large spheres ($x >> 1$) and plane wave illumination. But the limitations of such approaches are

also evident. A complete analysis valid for all parameter ranges calls for an exact Lorenz-Mie theory. In what follows, we briefly recall the essential steps associated with Lorenz-Mie theory [11]. This is done more to bring out role and importance of the Mie coefficients, which surface now and again in most of the problems. These can be as varied as extinction or QED aspects of decay rate modification of atoms or energy transfer between them.

Let the microsphere be illuminated by a *x*-polarized plane wave propagating along the *z*-direction. In view of the spherical symmetry of the scatterer the incident wave needs be decomposed in the vector spherical harmonics $\vec{M}_{o1n}^{(1)}$ and $\vec{N}_{e1n}^{(1)}$ as follows

$$\vec{E}_i = \sum_{n=1}^{\infty} E_n \left( \vec{M}_{o1n}^{(1)} - \vec{N}_{e1n}^{(1)} \right), \quad E_n = \frac{i^n E_0 (2n+1)}{n(n+1)}, \tag{2}$$

where $E_0$ is the incident field amplitude. Similarly the internal and scattered fields can also be expanded as

$$\vec{E}_1 = \sum_{n=1}^{\infty} E_n \left( c_n \vec{M}_{o1n} - i d_n \vec{N}_{e1n} \right), \tag{3}$$

$$\vec{E}_s = \sum_{n=1}^{\infty} E_n \left( i a_n \vec{N}_{o1n}^{(1)} - b_n \vec{M}_{e1n}^{(1)} \right), \tag{4}$$

respectively. The vector spherical harmonics in Eqs.(2)-(4) are given by

$$\vec{M}_{\begin{pmatrix} e \\ o \end{pmatrix}_{mn}} = \mp \frac{m}{\sin\theta} j_n(kr) P_n^m(\cos\theta) \begin{pmatrix} \sin \\ \cos \end{pmatrix} m\phi \hat{\theta} - j_n(kr) \frac{\partial P_n^m}{\partial \theta} \begin{pmatrix} \cos \\ \sin \end{pmatrix} m\phi \hat{\phi}, \tag{5}$$

$$\begin{aligned} \vec{N}_{\begin{pmatrix} e \\ o \end{pmatrix}_{mn}} &= \frac{n(n+1)}{kr} j_n(kr) P_n^m(\cos\theta) \begin{pmatrix} \cos \\ \sin \end{pmatrix} m\phi \hat{r} \\ &+ \frac{1}{kr} [krj_n(kr)]' \left[ \frac{\partial P_n^m}{\partial \theta} \begin{pmatrix} \cos \\ \sin \end{pmatrix} m\phi \hat{\theta} \mp \frac{m}{\sin\theta} P_n^m(\cos\theta) \begin{pmatrix} \sin \\ \cos \end{pmatrix} m\phi \hat{\phi} \right]. \end{aligned} \tag{6}$$

The vector functions $\vec{M}^{(1)}$ and $\vec{N}^{(1)}$ are obtained from Eqs.(5),(6) by replacing $j_n$ by $h_n^{(1)}$. The internal (external) Mie coefficient $c_n, d_n$ $(a_n, b_n)$ can be evaluated by satisfying the standard boundary conditions of continuity of the tangential components of the electric and magnetic fields at $r = a$. This yields, for example, for $a_n$ and $b_n$, the following

$$a_n = \left[\left(D_n(\overline{m}x)/\overline{m} + n/x\right)\psi_n(x) - \psi_{n-1}(x)\right]/A, \tag{7}$$

$$b_n = \left[\left(\overline{m}D_n(\overline{m}x) + n/x\right)\psi_n(x) - \psi_{n-1}(x)\right]/B, \tag{8}$$

where the denominators *A* and *B* are given by

$$A = \left(D_n(\overline{m}x)/\overline{m} + n/x\right)\xi_n(x) - \xi_{n-1}(x), \tag{9}$$

$$B = \left(\overline{m}D_n(\overline{m}x) + n/x\right)\xi_n(x) - \xi_{n-1}(x), \tag{10}$$

In Eqs.(7)-(10) , $\psi_n, \xi_n$ are the Ricatti Bessel functions and $D_n$ is the logarithmic derivative [11]. Note that the internal field coefficients (expressions not given here) have the same denominators $A$ and $B$, respectively. In terms of the scattered field coefficients, the extinction coefficient $Q_{ext}$ is given as

$$Q_{ext} = \frac{2}{k^2 a^2}\sum_{n=1}^{\infty}(2n+1)\,\mathrm{Re}(a_n + b_n) \tag{11}$$

It is clear from Eq.(11), (7) and (8) that resonances in extinction will occur at the zeroes of *A* (*B)* which will be accompanied by the enhancement of the external as well as the internal field coefficients $a_n, d_n$ $(b_n, c_n)$. Moreover, since $b_n$ is associated with $\vec{M}$ (see Eq.(4) with no radial component of electric field, it is natural to call the corresponding resonance as a TE (transverse electric) mode. On a similar footing TM (transverse magnetic) modes can be associated with the poles of $a_n$ (zeroes of *A*). Thus the

dispersion relation for the TE and TM modes are given by $B = 0$ and $A = 0$, respectively. A close look at any of these dispersion equations reveals that for a given mode number $n$ there can exist several zeroes of the dispersion equation. These zeroes (and the corresponding modes) originating from the oscillations of the Bessel function are labeled by the order number $l$. Since the radial distribution is given by the spherical Bessel functions $j_n$ or their derivatives, $l$ represents the number of nodes in the radial distribution. Thus $l$ determines the number of intensity peaks in the radial distribution inside the sphere. The physical meaning of $n$ is clear even from Eq.(1). It gives half the number of intensity maxima along the great perimeter of the sphere. Thus in the simplest possible case of a perfect sphere the mode resonances can be labeled by two integers, *viz.* mode number $n$ and order number $l$. A typical extinction feature for a water droplet is shown in Fig.1a where each peak is labeled by the corresponding mode.

We now pay attention to some of the relevant and salient features of these modes which are listed below

A. **Extra high quality factor**: These modes, especially for large $n$, (correspondingly large $x$ (from Eq.(1)) and low $l$, possess extraordinarily high quality factors. Some of the very first experiments reported a quality factor of $10^8$ in the optical domain [16]. Recently a quality factor of a $10^{10}$ in the visible range has been reported [12]. Possibility of achieving a quality factor of $10^{12}$ has also been pointed out [21]. We need to stress here that in a standard Fabry-Perot cavity one needs to have finesse of the order of $10^8$ in order to achieve such quality factors ($\sim 10^{10}$), which is quite challenging from an experimental angle.

B. **Localization of the internal fields and large local field enhancements**: It was mentioned earlier, that the internal radial field distribution is given by the spherical Bessel functions $j_n's$ or their derivatives. As a consequence, for large *n* (in large spheres) and for lower order modes the resonant field is localized near the edge of the microsphere. The radial distribution is confined [22] mostly in the region $\frac{a}{\overline{m}} \le r \le a$ (see Fig.1b). The localization of the field at resonance leads to large local field enhancements. A typical high-Q mode, namely, $a_{2312,167}$ mode of a silica sphere (with $\overline{m} = 1.46$) of radius $a = 200\mu m$ was shown to lead to an enhancement by six orders of magnitude[23]. The implications of such local field enhancements for the purpose of nonlinear and quantum optics are obvious. Atoms or molecules placed near the antinodes of the field will experience large fields resulting in 'zero' threshold optical processes. In fact, lasing, bistability and wave mixing have all been reported which exploit this property of the WGM. The role of WGM's as a probe for the strong interaction regime of cavity QEDs was also pointed out.

Till now we have been discussing the case of perfect spheres. A lot of activity has been devoted to the case when the spheres are deformed. For deformed spheres a third quantum number, namely, *m* comes into play. A perfect sphere has all the *m*-modes degenerate with $2n+1$ fold degeneracy. For axisymmetric deformation (viz. for prolate or oblate spheroids) the degeneracy is partially lifted leading to distinct frequencies for *m* values $\pm n, \pm(n-1), ..,\pm 1, 0$. The plus (minus) refers to the counter clockwise (clockwise) modes. Note that in perfect spheres or spheres with axisymmetric deformation the degeneracy of the clockwise and counter clockwise modes (also known as Kramer's

degeneracy) are still present. In a recent beautiful experiment this degeneracy was shown to be lifted by the inhomogeneities of a sphere [24] with eccentricity $10^{-3}$. A stabilized diode laser radiation was coupled into the sphere through a prism coupler. Both forward and backward scattered light was monitored and was shown to lead to well defined splitting. However, the eccentricity leading to the lifting of the degeneracy of the $|m|$ modes (with spacing 500MHz) was not the source of splitting which was just few hundred kHz. The splitting resulting from the lifting of Kramer's degeneracy was explained in terms simple-minded model of coupled oscillators depicting the counter propagating modes.

We now comment on the computational difficulties associated with Mie scattering, especially for large spheres. For large size parameters $x$ the convergence of the infinite series giving the extinction coefficient or other relevant physical quantities can pose a nontrivial problem [25]. Due to this and also with a motivation for gaining physical insight, a lot of research was directed towards developing approximate analytical expressions for the location, width and the strengths of the WGM's [26-30]. Some of them, especially the uniform approximation method of Guimaraes and Nussenzveig [30] needs to be mentioned due to their high accuracy at least for moderate size parameters ($x$~10).

## 3. Excitation and characterization of the WGM's

In the early days the WGM's were excited basically by coupling in the radiation using a prism coupler, much like in waveguide geometries. The evanescent wave in the gap between the prism and the sphere results from total internal reflection of the incident wave off the base of the prism. For proper angles of incidence and the frequency of the incident radiation this is sufficient to couple selectively to some of the WGM's. Recent

techniques use the evanescent field of single mode optical fibers [31-34]. Generally the fiber is mounted on a flat substrate and side polished to expose the field of the propagating mode. For example, in some experiments the fiber [33] with a core radius $1.9\mu m$ was side polished to a thickness of $0.7\mu m$. Coupling efficiency is higher if the microsphere is embedded in a liquid that is index matched to the fiber cladding. The analysis of the fiber-microsphere system requires an extension of the standard Lorenz-Mie theory for plane wave illumination and is referred to as the generalized Lorenz-Mie theory [35]. In essence the fiber–microsphere system has a direct relevance to the problem of off-axis excitation of the sphere by a gaussian beam. It turns out that a resonant off-axis gaussian beam excites the WGM's of a microsphere more efficiently than does a plane wave [34].

For a very long time the assignment of the mode and order numbers to the experimentally observed peaks in extinction or scattering remained a formidable problem. Since the location and widths of the resonances are sensitive to deformation and many other factors, a correspondence of the experimental data with Mie calculation with just two parameters, namely, $x$ and $\overline{m}$ proved to be nontrivial [25]. Due to the phenomenal achievements in the near field optics, it is now possible to directly probe the intensity distribution due to the excitation of various WGM's and assign the corresponding quantum numbers [31,36]. In a nice experiment, Haroche and coworkers mapped the intensity pattern in a sphere with broken spherical symmetry [31]. Later they were able to assign the quantum number $n$ by looking at the standing wave pattern along the equator of the sphere. In both these experiments polished half-fiber were used to excite the WGM's. In the first experiment the source of broken spherical symmetry was the fiber stem, which was used for manipulating the position of the microsphere. Both the

experiments used the micron sized molten tip of a fiber as the near field probe. The idea of using the fiber tip as the near field probe was borrowed from an experiment [37], where the field inside a Fabry-Perot cavity was probed by folding the resonator on a total internal reflection prism and mapping the evanescent field on the prism surface. This tip was used as the aperture and placed in the evanescent field just outside the sphere. The tip was moved on the surface and the radiation collected by it was sent to the detector via the fiber channel. In the system with broken spherical symmetry single (polar) angular peak was observed for the $|m| = n$ mode. Number of observed peaks was given by $n - |m| + 1$ which was justified by an asymptotic expression for the angular pattern.

## 4. Scope of the WGM's: Lasing and Nonlinear Optics

In the foregoing we had stressed the extraordinary properties of the WGM's like their extra-high quality factor and associated large local field enhancement. These have found immediate applications in lasing, Raman scattering and nonlinear optics. In fact, the very first report, which showed a quality factor $10^8$, had demonstrated the bistable response and indicated the possible use of microspheres as logic elements [16]. A vast amount of research has been devoted to lasing mostly in liquid droplets, because of the simplicity of generating these droplets by vibrating orifice aerosol generators. A proper doping by a suitable dye and pumping by another laser led to "zero effort" lasing. The main drawback of the droplet lasers is that the whole surface of the drop lases leading to the loss of one of the major useful properties of the standard lasers, namely, the directionality. In order to avoid this problem Micro disk lasers have been proposed and realized using semiconductor heterostructures [38]. These have been shown to be efficient low threshold

integrated sources, much needed by industry. Most of the work on liquid droplet systems is now well-documented [13-15]. In view of the aforesaid, we review some of the important work on solid-state systems, which shows the current trend with definite potential for device application. Perhaps the first systematic and thorough investigation of a solid-state microsphere laser was carried out by Baer [39]. Continuous wave lasing was reported in a ground and polished single crystal of Nd-YAG microsphere with diameter 5mm. Gonokami et al. carried out a considerable amount of research on dye doped polystyrene microspheres [40]. They used modern fiber probes to monitor the radiation. Polystyrene spheres with diameter ranging from $10\mu m$ to $92\mu m$ were doped with nile red and pumped by a 520 *nm* nanosecond pulsed dye laser. For low pump powers, the emission spectrum was broad with no distinctive features. An increase in pump power led to sharp lines in the emission due to many of the WGM's, both TE and TM. The rim of the sphere was shown to be brighter than the center for pump levels above threshold. A minor modification of this experimental arrangement allowed Gonokami et al.[41] to show the remarkable possibility of the microsphere to be the 'atomic' constituents in an 'optical molecule' (see below). Yet in a remarkable experiment by the Haroche's group a very low threshold ($30\mu W$) green lasing at $540nm$ was reported very recently [42]. The $Er^{+3}$ doped silica or ZBLAN microspheres with diameters ranging between $60-120\mu m$ were fabricated by melting using a plasma torch (for ZBLAN) or a $CO_2$ laser (for silica). The microspheres were attached to the end of a fiber for easy manipulation. Cascaded transitions using a IR beam of a diode laser at 801 *nm* was used for pump which was coupled to the pump WGM through a prism coupler. The fluorescence studies revealed much different life times for ZBLAN (0.55 *ms*) and silica (700 *ns*) for the lasing $^4S_{3/2}$

level. This explained the observed effect of lack of lasing in $Er^{+3}$ doped $SiO_2$ For the ZBLAN microspheres a linear dependence of the output green radiation was noted as the absorbed pump power was varied. From the break of the curve, the threshold was estimated to be 30μW. Note that this threshold is about 300 times lower than the lowest in $Er^{+3}$ and 100 times lower than any previously reported IR to visible laser in any material.

It was mentioned earlier that there have been extensive studies on nonlinear optical effects like optical bistability, wave mixing, Raman scattering (both spontaneous and stimulated) etc. Here we make a brief mention of some of the really low threshold experiments exploiting the high quality factor (Q ~ $10^9$) and small mode volume ($\sim 300\lambda^3 \sim 150\,\mu m^3$). Kerr bistability with a very nominal threshold of few microwatts was observed in a recent experiment [43]. A variety of stimulated optical processes (stimulated Raman scattering and four-wave mixing) under relatively low cw power in liquid droplets [4] were demonstrated. The low threshold power (e.g. 30 W/cm$^2$ for SRS) for these processes was attributed to the cavity QED enhancements (>100 times) of the nonlinear coefficients. The role of QED enhancement can be appreciated if one notes that these effects are observable in bulk samples only under intense nanosecond pulse excitations. Considerable theoretical efforts have gone in understanding the various nonlinear optical phenomena [see Ref.6 and references therein]. A recent theoretical proposals [44] deals with the possibility of the soliton propagation in a large totally reflecting microsphere. In the anomalous dispersion regime, the corresponding propagation equations are reduced to a nonlinear Schrödinger equation with a loss term, which is identical to that for a nonlinear lossy fiber. Thus possibility of bright soliton

propagation is predicted when the size of the sphere is constrained to support only one radial mode. Another interesting theoretical observation addresses the issue of the existence of the nonlinear lasing modes [45] in micro disks with nonlinear polarization modeling the nonlinear response of the lasing medium.

## 5. Weak coupling Regime of Cavity QED.

It is often a common misunderstanding that the features of an atom like spontaneous emission rate and the frequency shift are its inherent properties. In fact, there is nothing sacred about them since they are manifestations of atom-vacuum coupling. They would be meaningless if there were no vacuum fluctuations. Once this is appreciated, tailoring of the vacuum fluctuations is bound to lead to an atom with changed decay rate and energy shift. A quantitative measure of the properties of vacuum is the photon density states which for extended media is given by the smooth function

$$\rho_v(\omega) = \frac{\omega^2}{\pi^2 c^3}. \qquad (12)$$

In a cavity the density of states consists of peaks at the resonance frequencies with half-width $\Delta\omega \sim 1/\tau$, where $\tau$ is the lifetime of the cavity mode. As mentioned in the introduction, in the weak coupling limit (as in a bad cavity) when the leakage of the photon dominates over reexcitation of the atom, one can apply Fermi golden rule, modified by replacing the vacuum density of states $\rho_v(\omega)$ by a position dependent cavity density of states $\rho_c(\omega, \vec{r})$ [1]. Thus the transition probability for atoms in a cavity is given by

$$\Gamma_c = \frac{2\pi}{\hbar^2}|d|^2 \rho_c(\omega,\vec{r}). \qquad (13)$$

Since the measured rate is mostly for a collection of atoms a spatial averaging over the cavity volume $V$ is needed to arrive at the cavity density of states $\rho_c(\omega)$. The modification of the decay rate is then given by the ratio of the transition rate $\Gamma_c$ to that of free space $\Gamma_o$ (same as $\Gamma_c$ except that $\rho_c$ replaced by $\rho_v$) or the ratio of the corresponding density of states. One thus has an enhancement of the spontaneous emission at cavity resonance frequencies, which are associated with the peaks of the cavity density of states. On the other hand spontaneous emission will be inhibited where there are no photon modes e.g., in a planar cavity below cut off (length of the cavity is less than half the wavelength of the transition). In the context of planar geometries a large number experiments has been performed [1,2,5,46-51], which clearly demonstrated the enhancement/inhibition features. A lot of attention was paid to microcavities (with length L ~ $\lambda$). It was shown that a $\lambda/8$ ($\lambda/2$) cavity leads to inhibition (enhancement) of spontaneous emission [46]. In a later study 'zero- threshold' lasing was demonstrated in a $\lambda/2$ cavity while a $5\lambda$ cavity exhibited a pronounced threshold behavior [5].

In the context of microspheres it was shown by several authors that in the weak interaction regime modified Fermi Golden rule can be applied. Since the theoretical issue lacks major controversies we pay attention to some early but classic experiments with liquid droplets [18]. The experiment was performed with a linear stream of droplets doped with chelated Eu ions. The excitation beam was focused to one drop at a time creating an excited $Eu^{+3}$ population concentrated near the droplet rim. By imaging the droplets at various distances as they fall, the temporal evolution of the $Eu^{+3}$ spectral emission was

sequentially mapped. Sharp WGM features on a broad fluorescence background were noted. For a $24\,\mu m$ diameter sphere, both these features were shown to decay at the free space rate. However, for a $10\,\mu m$ diameter droplet the WGM features decayed more quickly (2.5 times) and the background decayed more slowly (1.5 times) than free space $Eu^{+3}$ ion excitation. In order to understand the absence of rate modification for the larger droplet, a careful analysis of Purcell's formula was carried out and the three relevant frequency scales were identified. These turned out to be the emission bandwidth $\delta\nu_{HB}$, spectral width of the WGM $\delta\nu_{WGM}$ and the mode spacing (for same order *l*) $\Delta\nu_{WGM}$ is inversely proportional to radius *a* and its asymptotic expression is given by

$$\Delta\nu_{WGM} = \tan^{-1}\sqrt{\overline{m}^2 - 1}\Big/\left(2\pi a\sqrt{\overline{m}^2 - 1}\right). \qquad (14)$$

If $\delta\nu_{HB} > \Delta\nu_{WGM}$ (i.e., the emission spectrum is broad enough to cover several whispering gallery modes, there is practically no lifetime change. It was shown that in the intermediate regime $\Delta\nu_{WGM} > \delta\nu_{HB} > \delta\nu_{WGM}$ the enhancement factor reduces to $\Delta\nu_{WGM}/\delta\nu_{HB}$. Thus droplets with narrow homogeneous width $\delta\nu_{HB} < \Delta\nu_{WGM}$ could exhibit lifetime changes. Each WGM with width narrower than the emission profile contributes equally to the Purcell integral since the product of spectral width $(\sim 1/Q)$ and the peak density per mode $(\sim Q)$ is a constant. Hence the intermediate regime is characterized by an absence of the dependence on quality factor of the modes. Experiments on enhancement/inhibition of spontaneous emission in solid-state systems have also been performed. Wang et al [19] used a Nd-glass microsphere near the 890 *nm* band. They noted considerable differences in the emission spectra depending on whether the central part or the rim of the sphere was excited. Location dependent enhancement of

spontaneous rate reaching a maximum of $10^3$ times the free space value was reported. New lasing lines at 890 *nm* were also observed.

## 6. Strong interaction regime of cavity QED: Vacuum Rabi splitting:

In the previous section we considered the interaction of the atomic system with a 'bad' cavity, where issues related to enhancement/inhibition could be settled by using Purcell's formula. It is clear that for high-Q modes application of Fermi Golden Rule is no more justified. Longevity of the photon in the cavity allows it to re-excite the atom leading to the periodic exchange of the energy between the atom and the cavity mode. This periodic exchange results in the vacuum field Rabi splitting [7-9]. The phenomenon of splitting can easily be understood if one uses a resonant absorber as the atomic system and takes a Fabry-Perot cavity as the other constituent [10,52]. Let the resonant absorber be characterized by the dielectric function $\varepsilon(\omega)$ which has a resonance at $\omega_0$ with half-width $\gamma_0$ and can be written as follows

$$\varepsilon(\omega) = \varepsilon_0 + \frac{\omega_p^{\,2}}{\omega_0^{\,2} - \omega^2 - 2i\gamma_0\omega} \tag{14}$$

In Eq. (12), the plasma frequency $\omega_p$ can be related to the number density and the dipole matrix elements of the atoms. The modes of the cavity with mirror reflection coefficient *r* can be determined from the dispersion relation given by

$$1 - r^2 e^{2ikL} = 0, \; k = \frac{\omega}{c}\sqrt{\varepsilon(\omega)}, \tag{15}$$

where *L* is the length of the cavity. The mirrors of the cavity were assumed to be identical and loss less. Let the atoms be resonant with one of the empty cavity resonances i.e., let

$\omega_c = \omega_0$ ( $\omega_c$ is given by $\frac{\omega_c}{c}\sqrt{\varepsilon_0}\, L = m\pi$ with integer $m$). The roots of Eq.(15) are given by

$$\omega = \omega_0 \pm \frac{\omega_p}{2} - i\frac{\kappa + \gamma_0}{2}, \tag{16}$$

where $\kappa$ is the half width of the cavity resonance. In writing Eq.(14) we assumed that $\omega_0 >> \omega_p >> \kappa$. The splitting given by Eq.(14) brings out two salient features, namely,

(a) The splitting is proportional to $\omega_p$ which in turn depends on the square root of the number density of the atoms. This is consistent with the quantum results [9].

(b) The split resonances have line width equal to the averages of the two rates $\kappa$ and $\gamma_0$. Thus one can have subnatural line width $\sim \gamma_0/2$ if $\kappa << \gamma_0$.

Analogous arguments can be successfully extended to cavities with other geometries, in particular to microspherical cavities [17,23,10]. A detailed and exact calculation was launched for the extinction of microspheres doped with resonant absorbers to show the vacuum Rabi splittings for modes with moderate Q (using $b_{56,2}$, $b_{61,1}$ modes of water droplets) as well as high-Q modes ( $a_{2312,167}$ mode of a silica microsphere) The results for $a_{2312,167}$ are shown in Fig.2 where we have plotted the extinction coefficient as functions of detuning for two values of the atomic decay. It is clear from these curves that with an increase in the density of the dopants ($\sim\omega_p^2$) the amount of splitting increases. The corresponding dispersion equations were solved exactly for the locations and the widths of the split modes. It was shown that splitting could be achieved at very nominal densities of the dopant atoms for high-Q modes like $a_{2312,167}$. Effects of small frequency mismatch

between the atom and cavity resonances was studied and was shown to lead to asymmetry in the split extinction profiles.

There have been several experimental observations of the vacuum Rabi splitting, most of them involving planar microcavities [52-55]. Some of the recent studies are centered on quantum wells or inorganic/organic semiconductor microcavities [56-60]. A giant splitting of 160 meV was reported at room temperature using a Zn-porphyrin derivative[59]. A very interesting polariton induced optical asymmetry was found in a coupled semiconductor microcavities [60].

## 7. Quantum electrodynamic effects mediated by whispering gallery modes: A general approach for both weak and strong coupling regimes

As was mentioned earlier a large number of interesting and important effects arise as a result of the interaction of the vacuum of the electromagnetic field and matter. These include the life times of the excited atomic and molecular states, radiative shifts of the energy levels, van der Waal forces, dipole-dipole interactions etc. These effects have been extensively studied. In this section we bring out the remarkable effects of the presence of a medium particularly when the medium supports natural modes of oscillation, which are in addition very long lived. The latter is the case when the medium is in the form of a sphere. This is because the medium supports whispering gallery modes many of which can have very high Q value. In what follows, we will present an outline of our calculation of such effects and present some of the more important results.

A standard approach to the calculation of the QED effects [62] requires (a) quantization of the electromagnetic field in presence of a finite medium, (b) application of the time

dependent perturbation theory. For the purpose of simplicity we do not go through the quantization route. Instead, we use classical equations of motion, which capture all the essential physics [3,62,63]. We then use a kind of translation rule to get the corresponding QED results. In our approach the key quantity is the dyadic Greens function $\vec{\vec{G}}(\vec{r}_A, \vec{r}_B, \omega)$. Furthermore, the approach based on the equations of motion also enables us to go to the nonperturbative regime of electrodynamic interactions.

Let us consider the specific geometry shown in Fig.3. Here we have two dipoles similarly oriented and located on the two sides of a sphere. Let $\omega_0$ be the frequency of oscillation of each dipole unperturbed by any interaction. Let us examine the net electromagnetic field at say the position of the dipole *A*. The field consists of two contributions, namely, (a) the self field, i.e., the field produced by the dipole *A* at its own position, (b) the field produced by the dipole *B* at the position *A*. Note that each of these fields depend on the presence of the medium. Further note that each of these fields can be calculated in terms of the dyadic Greens function, which contains all the information on the properties and the geometry of the medium. They are to be calculated from the corresponding wave equations subject to the proper boundary conditions. Due to the presence of the source, like in any linear inhomogeneous problem, $\vec{\vec{G}}$ can be broken up in two parts: the translationally invariant solution $\vec{\vec{G}}^{(0)}$ and the boundary contributions $\vec{\vec{G}}^{(s)}$. Thus $\vec{\vec{G}}$ can be written as[61,64]

$$\vec{\vec{G}} = \vec{\vec{G}}^{(0)} + \vec{\vec{G}}^{(s)}, \tag{17}$$

where $\vec{\vec{G}}^{(0)}$ and $\vec{\vec{G}}^{(s)}$ satisfy the following equations

$$\vec{\nabla} \times \vec{\nabla} \times \vec{\vec{G}}^{(0)}(\vec{r}, \vec{r}', \omega) - \frac{\omega^2}{c^2} \varepsilon_0 \vec{\vec{G}}^{(0)}(\vec{r}, \vec{r}', \omega) = 4\pi \vec{\vec{I}} \delta(\vec{r} - \vec{r}'), \tag{18}$$

$$\vec{\nabla}\times\vec{\nabla}\times\vec{\vec{G}}^{(s)}(\vec{r},\vec{r}',\omega)-\frac{\omega^2}{c^2}\varepsilon_0\vec{\vec{G}}^{(s)}(\vec{r},\vec{r}',\omega)=0\ . \tag{19}$$

Let us stress that Eq.(19) being a homogeneous equation has solutions with unknown coefficients, which are to be determined from the boundary conditions. Thus the information about the environment (boundaries) enters through these coefficients. Modification of the environment leading to resonance enhancement of any of these coefficients will lead to dramatic changes in the response of the dipolar system. Note also that free space Green's function lacks any resonant features and its effect can be incorporated through introducing the decay rate and the renormalized oscillation frequency.

The literature on Green's function is really vast and they have been calculated for various planar and spherical geometries [61,64-66]. We restrict ourselves only to the case of microspheres for which the surface component of the Green's function is given by [64]

$$\begin{aligned}\vec{\vec{G}}^{(s)}(\vec{r}_A,\vec{r}_B,\omega) = -ik_0\sum_{n=1}^{\infty}\sum_{m}(2-\delta_{m,0})\frac{(2n+1)(n-m)!}{n(n+1)(n+m)!}\\ \times[\vec{M}^{(1)}_{\binom{e}{o}_{mn}}(k_0\vec{r}_B)\,\vec{M}^{(1)}_{\binom{e}{o}_{mn}}(k_0\vec{r}_A)b_{\binom{e}{o}_n}\\ +\vec{N}^{(1)}_{\binom{e}{o}_{mn}}(k_0\vec{r}_B)\,\vec{N}^{(1)}_{\binom{e}{o}_{mn}}(k_0\vec{r}_A)a_{\binom{e}{o}_n}]\end{aligned}\ . \tag{20}$$

Note that the same Mie coefficients as in Eqs.(7) and (8) figure in Eq.(20).

Let us now analyze the role of Green's function in the radiative characteristics of the dipoles. A dipole oscillating at the frequency $\omega$ and located at the point *B* produces a field at the position, say, *A*

$$\vec{E}(\vec{r}_A,\omega)=\frac{\omega^2}{c^2}\vec{\vec{G}}(\vec{r}_A,\vec{r}_B,\omega)\cdot\vec{p}_B\,. \tag{21}$$

Remember that in case of arbitrary time dependence of the dipole one could do a Fourier analysis and use the relation (21) for each Fourier component. This is important, as even when we start a dipole at the frequency $\omega_0$, it will develop new frequency components as a result of interaction with the fields mentioned above. Thus a complete theory should treat such time dependences in a consistent manner and it is best to work in Fourier domain. Thus we define $\vec{p}_j(\omega)$ (*j=A, B*) as Fourier transform of $\vec{p}_j(t)$, i.e., for a dipole with frequency $\omega_0$ one will write $\vec{p}_j(\omega) = p_j \vec{n}_j \delta(\omega_0)$, where the unit vector $\vec{n}_j$ gives the orientation of the dipole. Clearly the system of two dipoles will satisfy coupled equations in the Fourier domain

$$\left(\omega_0^2 - \omega^2 - \frac{e^2\omega^2}{mc^2} G_{AA}(\omega)\right) p_A - \left(\frac{e^2\omega^2}{mc^2} G_{AB}(\omega)\right) p_B = 0, \qquad (22)$$

where

$$G_{ij}(\omega) = \vec{n}_i \cdot \vec{\vec{G}}\left(\vec{r}_i, \vec{r}_j, \omega\right) \cdot \vec{n}_j, \;\; i, j = A, B. \qquad (23)$$

The equation for the second dipole is given by Eq.(22) except for the replacement $A \leftrightarrow B$. The normal modes of oscillation are given by the roots of the dispersion equation which follows from Eq.(22)

$$\left(\omega_0^2 - \omega^2 - \frac{e^2\omega^2}{mc^2} G_{AA}(\omega)\right)\left(\omega_0^2 - \omega^2 - \frac{e^2\omega^2}{mc^2} G_{BB}(\omega)\right) - \left(\frac{e^2\omega^2}{mc^2} G_{AB}(\omega)\right)^2 = 0. \qquad (24)$$

Note that the Green's functions in Eqs.(22) and (24) include both the free space and the surface contributions. As mentioned earlier, the free space contribution can be incorporated by assuming a renormalized frequency $\omega_0$ and by introducing the free space decay rate $\gamma_0$ given by the following

$$\gamma_0 = \frac{e^2\omega}{2mc^2}\,\mathrm{Im}\left[G_{AA}^{(0)}(\omega)\right] = \frac{e^2\omega^2}{3mc^3}, \tag{25}$$

Note that the effects of free space interaction between the dipoles $G_{AB}^{(0)}$ can be implemented in the same vein or simply neglected for dipoles separated by many wavelengths. The surface contributions have a strong dependence on the geometry and for the specified system (see Fig.3), the relevant Green's functions are given by [62,64]

$$\begin{aligned} &-\frac{ie^2\omega}{2mc^2}G_{AA}^{(s)}(\omega) = \gamma_0(K_{AA} + i\Omega_{AA}) = \\ &= \sum_{n=1}^{\infty} -n(n+1)(2n+1)\frac{[h_n^{(1)}(k_0 r_A)]^2}{k_0^2 r_A^2}a_n, \end{aligned} \tag{26}$$

$$\begin{aligned} &-\frac{ie^2\omega}{2mc^2}G_{AB}^{(s)}(\omega) = \gamma_0(K_{AB} + i\Omega_{AB}) = \\ &= \sum_{n=1}^{\infty}(-1)^{n+1}n(n+1)(2n+1)\frac{h_n^{(1)}(k_0 r_A)h_n^{(1)}(k_0 r_B)}{k_0^2 r_A r_B}a_n. \end{aligned} \tag{27}$$

In Eqs.(26), (27) we separated out the imaginary and the real parts of the Green's function for convenience. We now emphasize that all the physics about radiative characteristics and their modifications due to the medium would be described by the solutions of Eq.(24). The solutions in turn would depend on the strength of interaction ($G_{AA}^{(s)}, G_{AB}^{(s)}$) enhanced by the natural modes of oscillation of the sphere (in our case by the a-modes).

We now consider specific cases pertaining to the various regimes. Consider a single dipole near the microsphere. The characteristic equation for this case follows from Eq.(24) and can be written as

$$\omega_0^2 - \omega^2 - 2i\gamma_0\omega\left[1 + K_{AA}(\omega) + i\Omega_{AA}(\omega)\right] = 0. \tag{28}$$

The solution to this equation will depend on the strength of the coupling of the dipole to the sphere. Let us first assume that the coupling is weak. Then we can ignore the frequency dependence of the Green's function in the neighborhood of the frequency $\omega_0$ replacing *K* and Ω by their values at $\omega_0$. In other words we assume that the solution of the full equation yields only a complex correction to $\omega_0$. We can further approximate $\omega_0^2 - \omega^2$ by $2\omega_0(\omega_0 - \omega)$. Then the result for the complex oscillation frequency becomes

$$\omega = (\omega_0 + \gamma_0 \Omega_{AA}(\omega_0)) - i\gamma_0 (1 + K_{AA}(\omega_0)). \quad (29)$$

It is clear from (29) that the real part of the Green's function Ω leads to frequency shift while the imaginary part *K* is responsible for the change in radiative decay. Analogous arguments can be extended to the case of two dipoles near the microsphere in order to determine the resonant energy transfer [67] between them.

In order to demonstrate the role of WGM's in enhancing the QED effects we carried out an extensive numerical study of the frequency dependence of the Green's functions [62]. Spheres of two radii, namely, 5 μm and 200 μm were chosen in order to compare the results for moderate and high Q WGM's. For the larger (smaller) sphere out of the variety of modes we selected $a_{2312,167}$ ($a_{39,1}$) mode with frequency $\omega_G$ = 1.8026933000486 $\mu m^{-1}$ (1.096835618 $\mu m^{-1}$) and quality factor Q = $1.28 \times 10^9$ ($1.22 \times 10^3$). The results for $K_{AB}$ and $\Omega_{AB}$ for equidistant dipoles ($d_1 = d_2 = d$) and $a_{2312,167}$ mode for two normalized distances, namely, $d/\lambda$ = 0.1 and 1.0 are shown in Fig.4b. The increasing distance of the dipoles from the surface leads to a significant reduction of the enhancement factor $K_{0AB} = \max(|K_{AB}|)$ from 1349.81 to 154.47. Note that single dipole enhancement factor $K_{0AA}$ has the same magnitude for the configuration under study. Analogous results for

$a_{39,1}$ mode are shown in Fig.4a. In contrast to the case of $a_{2312,167}$ mode, the enhancement factors for the same distances, i.e., $d/\lambda = 0.1$ and 1.0, are now reduced to 3.4 and 0.07, respectively. The distortion of the curves in Fig 4a is due to a nearby WGM $a_{44,1}$. These results clearly demonstrate that the dipole-dipole interaction, mediated by high Q WGM's like $a_{2312,167}$, can reach giant proportions. It is interesting to note that at such distances (>400 μm) the free space interaction between the dipoles is truly negligible.

As shown above the excitation of the extra high-Q WGM's can lead to giant enhancement in the Green's functions. In this regime it is necessary to take into the account the frequency dependence in the Green's dyadic. A close look at the frequency dependence as in the Fig.4b reveals that such resonances can be well approximated by a lorentzian characterized by the WGM resonance frequency $\omega_G$ and its half width $\kappa$. For example, the single point Green function (normalized to $\gamma_o$) can be broken up into the resonant (*R*) and the nonresonant (*N*) parts as

$$K_{AA} + i\Omega_{AA} = R(\vec{r}_A, \omega) + N(\vec{r}_A, \omega), \tag{30}$$

with the following dependence for the resonant contribution

$$R(\vec{r}_A, \omega) = \frac{\kappa f(\vec{r}_A, \omega)}{\kappa - i(\omega - \omega_G)}. \tag{31}$$

In Eq.(31) $f(\vec{r}_A, \omega)$ is determined by the spatial distribution of the mode and has a weak frequency dependence. Furthermore we assume that both *f* and *N* can be replaced by their values at resonance. Then Eq.(24) can be reduced to the following

$$\begin{aligned} &\left[(\Delta + i\gamma_0)(\Delta + i\kappa) + i\gamma_0 N_A(\Delta + i\kappa) - \gamma_0 \kappa f_A\right] \\ &\left[(\Delta + i\gamma_0)(\Delta + i\kappa) + i\gamma_0 N_B(\Delta + i\kappa) - \gamma_0 \kappa f_B\right] \\ &-\left[i\gamma_0 N_{AB}(\Delta + i\kappa) + (\Delta + i\kappa) - \gamma_0 \kappa f_{AB}\right]^2 = 0. \end{aligned} \tag{32}$$

In Eq.(32) $\Delta = \omega - \omega_G$ and the WGM was assumed to be in resonance with the dipole, i.e., $\omega_G = \omega_0$. Moreover, we used the abbreviations, say, $f_i = f(\vec{r}_i, \omega_o)$, $N_i = N(\vec{r}_i, \omega_o)$. The equation for the complex frequency correction for a single dipole near the microsphere can be obtained from Eq.(32) by setting $f_B = f_{AB} = 0$. The numerical results for a single dipole for both the modes $a_{39,1}$ and $a_{2312,167}$ are shown in Fig.5 . We have displayed both the real (solid line) and imaginary (dashed line) parts of Δ as functions of normalized distance from the microsphere. It is clear from Fig.5 that shorter distances lead to larger splittings in the frequency due to stronger interaction. In Fig.6 we have shown the frequency splittings in the case when both the dipoles (see Fig.3) interact via the microsphere. Clearly one now has four roots out of which the real parts of two almost coincide (the central branch) for the high-Q $a_{2312,167}$ mode (Fig.6b). Note that these modes are not degenerate since their imaginary parts are distinct (not shown).

In order to have some insight in the frequency splittings, we ignore the nonresonant contributions (which is quite justified for high–Q WGM's like $a_{2312,167}$). Under this approximation, and noting that $f_A f_B = f_{AB}^2$, the roots of Eq.(32) are given by

$$\Delta_1 = -i\gamma_0 \ , \quad \Delta_2 = -i\kappa$$
$$\Delta_{3,4} = \frac{-i(\gamma_0 + \kappa)}{2} \pm \sqrt{\gamma_0 \kappa (f_A + f_B) - \left(\frac{\gamma_0 - \kappa}{2}\right)^2} \, . \tag{33}$$

The first two roots give the bare atom or the bare cavity modes, the other two roots represent the manifestation of the d-d interaction. If the enhancement is not significant i.e. when

$$\gamma_0 \kappa (f_A + f_B) < \left(\frac{\gamma_0 - \kappa}{2}\right)^2 , \tag{34}$$

one has a modification of the decay rates from the average of the decay rates $(\gamma_0 + \kappa)/2$ In presence of large enhancements, when the inequality (34) is violated one has vacuum Rabi splitting, where the decay rate of both the split modes are characterized by the average of the two rates (see also Eq.(16) for the FP cavity). As is the case with most high-Q WGM's, the enhancements in the interaction is enough to lead to splittings at least for dipoles close to the surface. Thus the naturally given WGM's of a microsphere and the field enhancement associated with them are enough to lift the degeneracy of the atom–cavity system. We also note that the effect of a nearby mode (a typical example of such a resonance is the mode $a_{44,1}$ of a water droplet, which is very close to the mode $a_{39,1}$) can be incorporated in the same spirit by introducing another lorentzian. The presence of such a resonance (which is often the case with the WGM's of microspheres) leads to a mode repulsion effect.

## 8. Future Directions

Despite the considerable volume of theoretical research on the strong interaction regime in microspheres leading to vacuum Rabi oscillations, till now there is no experimental verification of the same. The difficulties that hindered experimental observation are mainly related to the complexity of the WGM spectra. It is clear that in spherical geometries it is extremely difficult to get a 'clean' mode spectrum like in Fabry-Perot cavities with length comparable or less than the wavelength. The other important reason has been the inhomogeneous broadening due to the spatial distribution of atoms. This can be reduced by laser cooling techniques. Since high-Q WGM's produce very small

evanescent field outside, strong coupling could be easier to observe with atoms on the surface or in the rim of the microsphere, where there is a large local field enhancement.

A deeper understanding of the exotic properties of the WGM's opened up possibilities for novel directions. Kimble and coworkers came up with the idea of atom galleries [68], whereby the atom revolves around dielectric microsphere. They showed that such motion is possible for three level atoms near the surface of the sphere with external two-frequency excitation. Another scheme for quasi-orbital motion was proposed by Klimov etal [69]. Here the vacuum field of the WGM is responsible for driving the ultra cold two level atom with arbitrary orientation of its dipole moment. Conditions for quasi-orbital motion was discussed in detail.

Another interesting area where research activities have just started is to probe the solitary wave solutions in nonlinear microspheres. A great deal of work needs to be done in order to find the nonlinear eigen modes of microspheres and their characteristics. Nonlinear mixing of the modes with orthogonal polarizations in deformed spheres pose yet another open question.

Perhaps the most interesting issue involves the fabrication of 'macroscopic' optical molecules. Gonokami and coworkers experimentally realized a tight-binding photonic molecule [41]. The molecule consisted of two dye doped polymer microspheres of diameter ranging from 2 to 5 μm. The bonding was via the coupling of the whispering gallery modes. The near perfect size control allowed for sufficiently narrow line width and large separation of the WGM's. Thus intricate and unwanted band mixing was avoided. Intersphere coupling constant was estimated to be larger than the WGM line width. This proved the feasibility of tight-binding hopping of light in a chain of connected

microspheres. Note that a similar goal of micro-manipulating the light path can be achieved in much more complicated systems having photonic band gap structures where the hopping is via the defect modes [70].

**Acknowledgements**

One of the authors (SDG) would like to thank the Department of Science and Technology, Government of India for supporting this work.

## Figure Captions

Fig.1. (a) Extinction coefficient $Q_{ext}$ as a function of frequency ω for a water droplet with $\overline{m} = 1.33$ and $a = 4.51\mu m$. Various peaks are marked by the corresponding WGM's. (b) Radial distribution for the $b_{56,2}$ and $b_{61,1}$ modes. Note the localization near the rim of the sphere.

Fig.2. $Q_{ext}$ as a function of detuning $\Delta\omega$ for $a_{2312,167}$ mode for various values of $\omega_p$. Curves 1,2 and 3 in (a) are for $\gamma_0$=4.0x10$^{-9}$ μm$^{-1}$, $\omega_p$=0.0 μm-1, 4.0x10$^{-9}$ μm-1 and 8.0x10$^{-9}$ μm-1. Curves 1,2 and 3 in (b) are for $\gamma_0$=1.0x10$^{-9}$ μm$^{-1}$, $\omega_p$=0.0 μm-1, 1.0x10$^{-9}$ μm-1 and 4.0x10$^{-9}$ μm$^{-1}$..

Fig.3. Schematic view of the microsphere of radius *a* with two similarly oriented dipoles on the z-axis, at distances of $d_1$ and $d_2$ from the surface of the microsphere. Refractive index of the sphere material is $\overline{m} = 1.46$, with vacuum as the outside medium.

Fig.4. Dipole-dipole characteristics $K_{AB}$ (solid line) and $\Omega_{AB}$ (dashed line) as functions of detuning $\omega_0 - \omega_G$ for $d/\lambda = 0.1$ for (a) $a_{39,1}$ mode and (b) $a_{2312,167}$ mode. Both the curves in (a) are normalized to the enhancement factor $K_{0AB} = \max(|K_{AB}|)$=3.4. The corresponding curves for $d/\lambda = 1.0$ are identical except that now $K_{0AB}$=0.07. The corresponding enhancement factors for (b) at distances $d/\lambda$=0.1 and 1.0 are 1349.81 and 154.47, respectively.

Fig.5. Real (solid line) and imaginary (dashed line) parts of the frequency correction $\Delta$ as functions of normalized distance $d/\lambda$ for a single dipole interacting with the WGM (a) $a_{39,1}$ and (b) $a_{2312,167}$.

Fig.6. Roots for the real part of the frequency correction as functions of normalized distance of the second dipole $d_2/\lambda$ for dipole-dipole interaction mediated by the WGM (a) $a_{39,1}$ and (b) $a_{2312,167}$. The first dipole is kept on the surface, i.e., $d_1$=0.0.

## REFERENCES


1. E.M. Purcell, Phys.Rev.**69**, 681 (1946).
2. D. Kleppner, Phys. Rev. Lett. **47**, 233 (1981).
3. S Haroche in *Fundamental Systems in Quantum Optics*, J. Dalibard and J. M. Raimond eds. (North Holland, Amsterdam, 1992). See also articles in *Cavity Quantum Electrodynamics*, P. Berman ed. (Academic, New York, 1994)
4. H.B. Lin and A.J. Campillo, Phys. Rev. Lett. **73**, 2440 (1994).
5. F. De Martini and G.R. Jacobovitz, Phys. Rev. Lett. **60,** 1711 (1988).
6. S.C. Hill and R.K. Chang, SPIE **1862**, 309 (1993).
7. J. Sanchez-Mondragon , N. B. Narozhny and J. H. Eberly, Phys. Rev. Lett. **51**, 550 (1983).
8. G. S. Agarwal, Phys Rev. Lett. **53**, 1732 (1984).
9. G. S. Agarwal, J. Opt. Soc. Am. **B2**, 480 (1985).
10. G. S. Agarwal, J. Mod. Opt.**45**, 449-470 (1998).
11. For general properties of whispering gallery modes, see, for example, C. F. Bohren and D. R. Huffman, *Absorption and scattering of light by small particles* (Wiley, New York, 1983).
12. M.L. Gorodetsky, A.A. Savchenkov and V.S. Ilchenko, Opt. Lett. **21**, 453 (1996).
13. M.H. Fields, J. Popp and R.K. Chang "Nonlinear Optics in microspheres" in "*Prog. in Optics",* ed. E. Wolf (North Holland, Amsterdam,1999) pp
14. S.C. Hill, R.E Benner and R.K. Chang, in *Studies in Classical and Quantum Nonlinear Optics,* ed. O. Keller (Nova Science, New York, 1995) p. 171.

15. S.C. Hill and R.E. Benner, in *Optical Effects Associated with Small Particles,* eds. P.W. Barber and R.K. Chang (World Scientific, Singapore, 1988) p.1.
16. V.B. Braginsky, M.L. Gorodetsky and V.S. Ilchenko, Phys Lett. **137**, 393 (1989).
17. G. S. Agarwal and S. Dutta Gupta, Opt. Commun. **93**, 173 (1992).
18. H.B. Lin, J.D. Eversole, C.D. Merit and A.J. Campillo, Phys. Rev. **A45,** 6756 (1992); A.J. Campillo, J.D. Eversole and H.B. Lin, Phys. Rev. Lett. **67**, 437 (1991).
19. Y.Z. Wang, B.L. Lu, Y.Q. Li and Y.S. Liu, Opt. Lett. **20**, 770 (1995).
20. S.K. Sarma and D.J. Somerford, "Scattering of light in the eikonal approximation", in *Progress in Optics,* ed. E. Wolf (North Holland, Amsterdam, 1999) **vol. 39**, pp 213-290. §3.
21. M.L. Gorodetsky, A.D. Prymakov and V.S. Ilchenko, Opt. Commn.(to appear).
22. J.L. Cheung, J.M. Hartings and R.K. Chang, in "*Handbook of Optical Properties* " **vol II**, eds. R.E. Hummel and P. Wibmann (CRC, New York, 1997) P. 233.
23. S. Dutta Gupta and G.S. Agarwal, Opt. Commn. **115**, 597 (1995).
24. D.S.Weiss, V Sandhoghdar, J. Hare, V. Lefevre–Seguin, J.M. Raimond and S. Haroche, Opt. Lett. **20**, 1835 (1995).
25. J.D. Eversole, H.B. Lin, A.L. Huston and A.J. Campillo, J. Opt. Soc. Am. **A7,** 2159 (1990).
26. C.C. Lam, P.T. Leung and K. Young, J. Opt. Soc. Am. **B9**, 1585 (1992).
27. S. Schiller and R.L.Byer, Opt. Lett. **16**, 1138 (1991).
28. H.M. Nussenzveig, in *Coherence and Quantum Optics* ed. J.H. Eberly *et al.* (Plenum, New York, 1990) P. 821.
29. L.G. Guimaraes and H.M. Nussenzveig, J. Mod. Opt. **41**, 625 (1994).

30. P.R. Conwell, P.W. Barber and C.K. Rushford, J. Opt. Soc. Am. **A1**, 62 (1984).

31. J.C. Knight, N. Dubreuil, V. Sandoghdar, J. Hare, V. Lefevre-Seguin, J.M. Raimond and S. Haroche, Opt. Lett. **20**, 1515 (1995).

32. A. Serpenguzel and S. Arnold, Opt. Lett, **21**, 695 (1995).

33. G. Griffel, S. Arnold, D. Taskent, A. Serpenguzel, J. Connolly and N. Morris, Opt. Lett, **21**, 695 (1986).

34. A. Serpenguzel, S. Arnold, G. Griffel and J.A. Lock, J. Opt. Soc. Am. **B14**, 790 (1997).

35. J.A. Lock and G. Gouesbet, J. Opt. Soc. Am. **A11,** 2503 (1994); G. Gouesbet and J.A. Lock, *ibid*, 2516 (1994).

36. J.C. Knight, N. Dubreuil, V. Sandoghdar, J. Hare, V. Lefevre-Seguin, J. M. Raimond and S. Haroche, Opt. Lett. **21**, 698 (1996).

37. D. Courjon, C. Bainier and F. Baida, Opt. Commn. **110,** 7 (1994).

38. S.L. McCall, A.F.J. Levi, R.E. Slusher, S.J. Pearton and R.A. Logan, Appl. Phys. Lett. **60**, 289 (1992).

39. T. Baer, Opt. Lett. **12**, 392 (1987).

40. M.K. Gonokami, K. Takeda, H. Yasuda and K .Ema, Jpn. J. Appl. Phys. **31**, L99 (1992); M.K. Gonokami, K. Ema and K. Takeda, Mol. Cryst. Liq. Cryst. **216**, 21 (1992).

41. T. Mukaiyama, K. Takeda, H. Miyazaki, Y. Zimba and M. K. Gonokami, Phys. Rev. Lett. **82**, 4623 (1999).

42. W. Von Klitzing, E. Jahier, R. Long, F. Lisillour, V. Lefevre-Seguin, J. Hare, J.M. Raimond and S. Haroche, J. Opt. **B**: Quantum Semiclass. Opt. **2**, 204 (2000).

43. F. Treussart, V.S. Ilchenko, J.F. Roch, J. Hare, V. Lefevre-Seguin, J.M. Raimond and S. Haroche, Eur. Phys J. **D1,** 235 (1998).

44. W.B. Whitten, M.D. Barnes, and J.M. Ramsey, J. Opt. Soc. Am. **B14,** 3424 (1997).

45. T. Harayama, P. Davis and K.S. Ikeda, Phys. Rev. Lett. **82**, 3803 (1999).

46. F. De Martini, G. Innocenti, G.R. Jacobovitz and P.Mataloni, Phys. Rev. Lett. **59**, 2955 (1987); F. De Martini, M. Marrocco, L. Crescentini and R. Loudon, Phys. Rev. Lett. **A43**, 2480 (1991).

47. Y. Yamamoto, S. Machida and G.Bjork, Opt. and Quantum Electron. **24**, S 215 (1992).

48. R.M. Amos and W.L. Barnes, Phys. Rev. **B55**, 7249 (1997); *ibid* **B59**, 7708 (1999); P.T. Worthing, R.M. Amos and W.L. Barnes, Phys. Rev. **A59**, 865 (1999); W.L. Barnes and P.T. Worthing, Opt. Commn. **162,** 16 (1999); W.L. Barnes, J. Mod. Opt. **45**, 661 (1998).

49. S.T. Ho, S.L. McCall and R.E. Slusher, Opt. Lett. **18,** 909 (1993).

50. A. Armitage, M.S. Skolmick, A.V. Kavokin, D.M. Whittaker, V.N. Astratov, G.A. Gehring and J.S. Roberts, Phys. Rev. **B58**, 15367 (1998).

51. D.G. Lidzey, D.D.C. Bradley, V. Virgili, A. Armitage, M.S. Skolmick and S. Walker, Phys. Rev. Lett. **82**, 3316 (1998).

52. Y. Zhu, D. J. Gauthier, S. E. Morin, Q. Wu, H. J. Carmichael and T. W. Mossberg, Phys. Rev. Lett. **64**, 2499 (1990).

53. R. J. Thompson, G. Rempe and H. J. Kimble, Phys. Rev. Lett. **68**, 1132, (1992).

54. M. G. Raijen, R. J. Thompson, R. J. Brecha, H. J. Kimble and H. J. Carmichael, Phys. Rev. Lett. **63**, 240 (1989).

55. F. Bernadot, P. Nussenzveig, M. Brune, J. M. Raimond and S. Haroche, Europhys. Lett. **17**, 33 (1992).

56. J Jacobson, S. Pau, H. Cao, G. Bjork and Y. Yamamoto, Phys. Rev. **A51**, 2542 (1995).

57. C. Weisbuch etal, Phys. Rev. Lett. **69**, 3314 (1992).

58. D. G. Lidgey, D. D. C. Bradley, T. Virgill, A. Armitage, M. S. Skolnik and S Walker, Phys. Rev. Lett. **82**, 3316 (1999).

59. D. G. Lidgey, D. D. C. Bradley, M. S. Skolnik, T. Virgill, S Walker and D. M. Whittaker, Nature, 395, **53** (1998).

60. A. Armitage, M. S. Skolnik, A. V. Kavokin, D. M. Whittaker, V. N. Astrakov, G. A. Gehring and J. S. Roberts, Phys. Rev. **B58**, 15367 (1998).

61. A general theory of cavity QED effects in presence of dielectrics or conductors is developed in G. S. Agarwal, Phys. Rev. **A11**, 230 (1975).

62. G. S. Agarwal and S. Dutta Gupta, in *Recent Advances in Atomic and Molecular Physics*, R Srivastava ed. (Phoenix, New Delhi, 2001) pp.1-13.

63. V.V. Klimov, M. Ducloy and V.S. Letokhov, J. Mod. Opt. **43,** 2251 (1996); V.V. Klimov, M. Ducloy and V.S. Letokhov, J. Mod. Opt. **44b** 1081 (1997); V.V. Klimov, and V.S. Letokhov, Phys. Rev. **A58,** 3235 (1998).

64. G. S. Agarwal and S. V. ONeil, Phys. Rev. **B28**, 487 (1983).

65. G. S. Agarwal and S. Dutta Gupta, Phys. Rev. **A57**, 667 (1998).

66. M. S. Tomas, Phys. Rev. **A51**, 2545 (1995); P. T. Leung and K. Young, J. Chem. Phys.89, 2894(1988);

67. S. Arnold, S. Holler and S. Druger, “The role of MDR’s in chemical physics: Intermolecular energy transfer in microdroplets” in *Optical Processes in Microcavities*, R. K. Chang and A. J. Campillo, eds. (World Scientific, Singapore, 1966).
68. H. Mabuchi and H.J. Kimble, Opt. Lett. **19**, 749 (1994); D.W. Vernooy, and H.J. Kimble, Phys. Rev. **A55**, 1239 (1997).
69. V. Klimov, V.S. Letokhov and M. Dudoy, Eur. Phys. J. **D5**, 345 (1999).
70. M. Bayindir, B. Temelkuran and E. Ozbay, Phys. Rev. **B61**, R11855 (2000);M. Bayindir and E. Ozbay, Phys. Rev. **B62**, R2247 (2000).

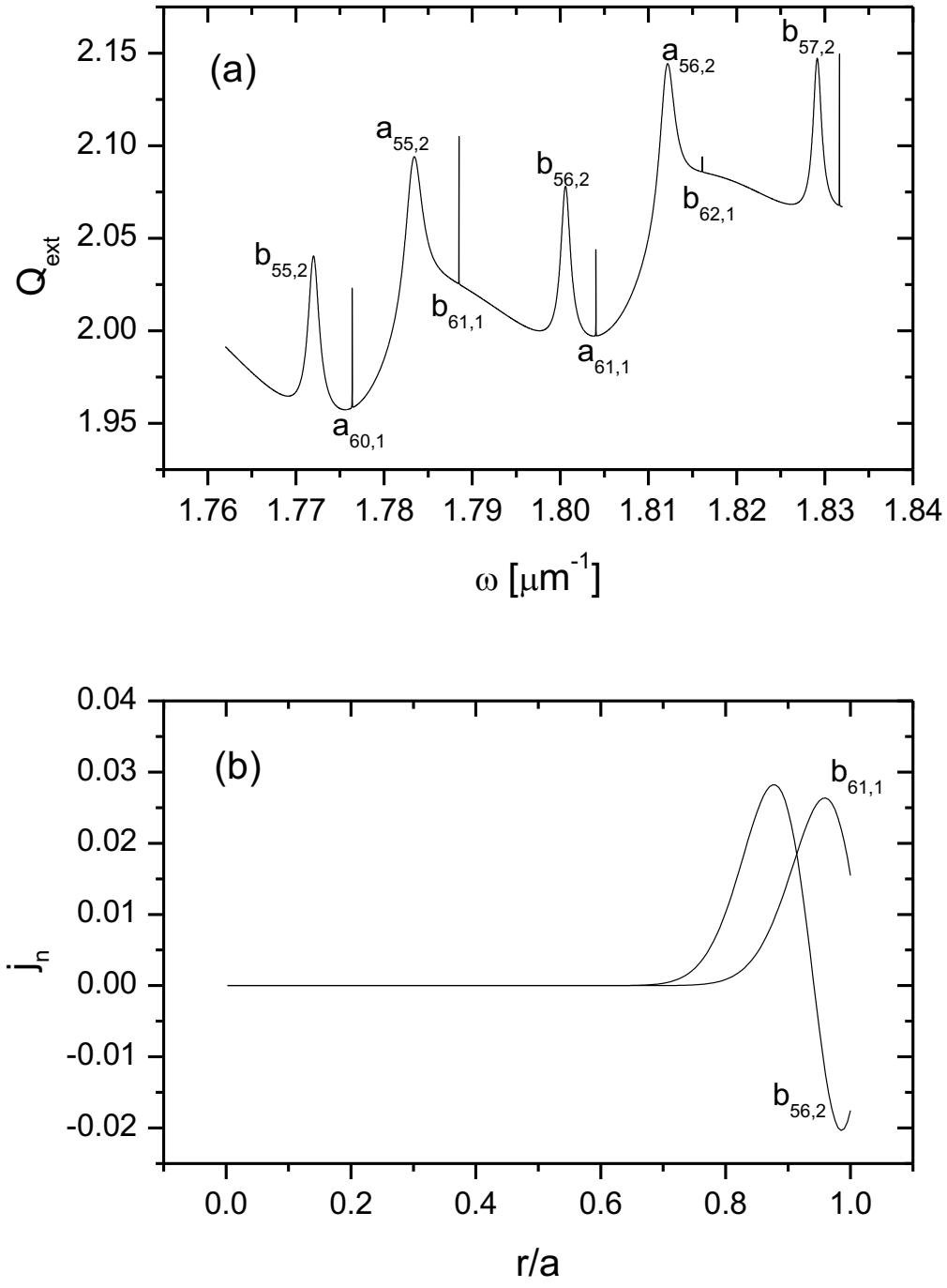


Fig.1 S Dutta Gupta and G S Agarwal, "Quantum optics & …"

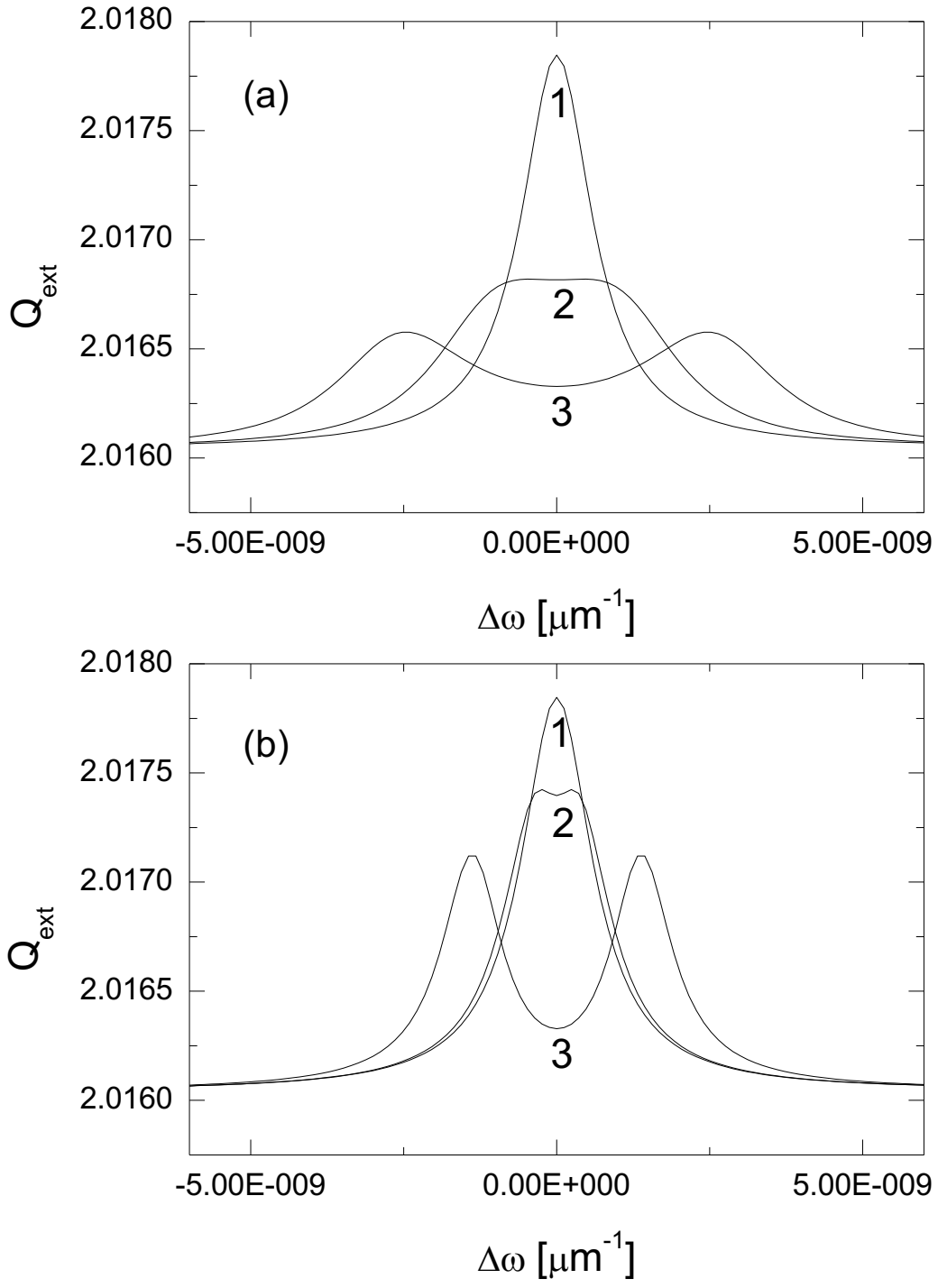


Fig.2 S Dutta Gupta and G S Agarwal, "Quantum optics & …"

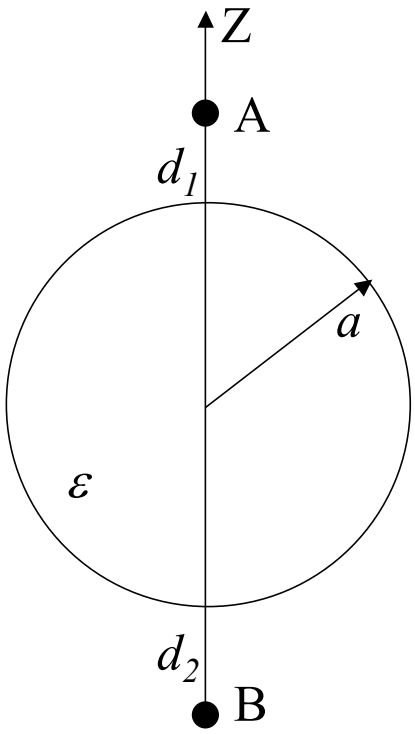


Fig.3 S Dutta Gupta and G S Agarwal,
"Quantum optics &…"

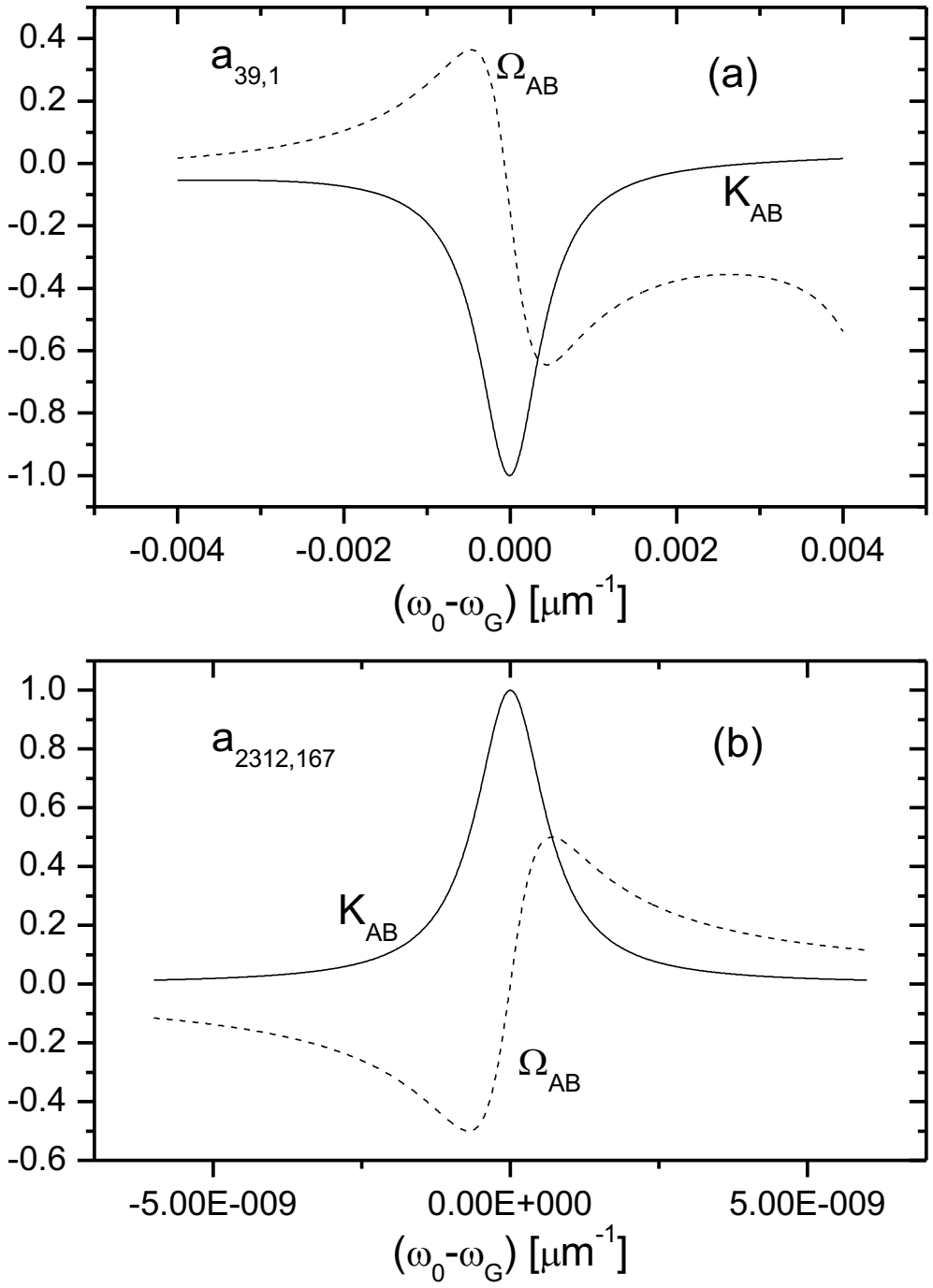


Fig.4 S Dutta Gupta and G S Agarwal, "Quantum optics & …"

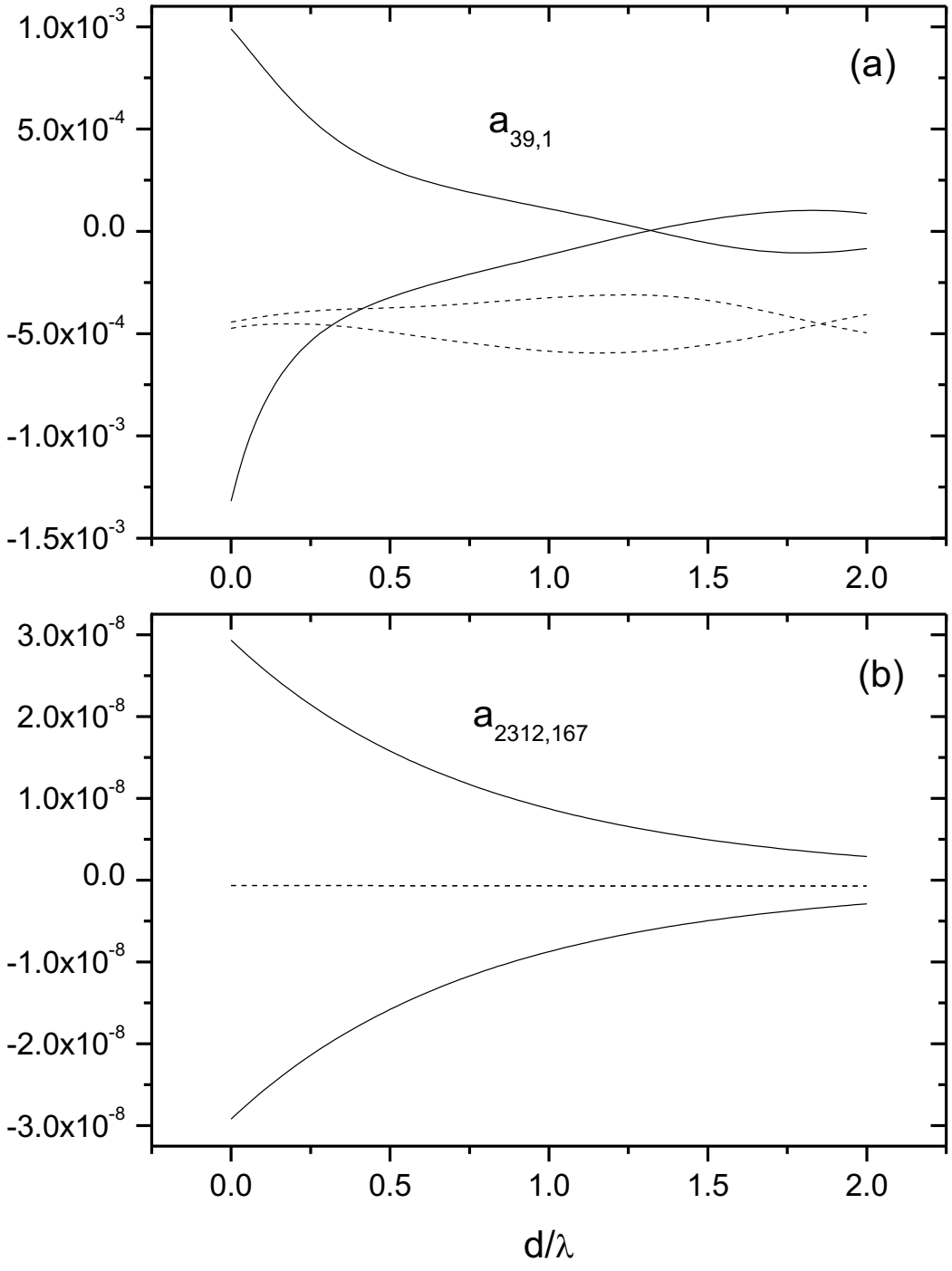


Fig.5 S Dutta Gupta and G S Agarwal, "Quantum optics & …"

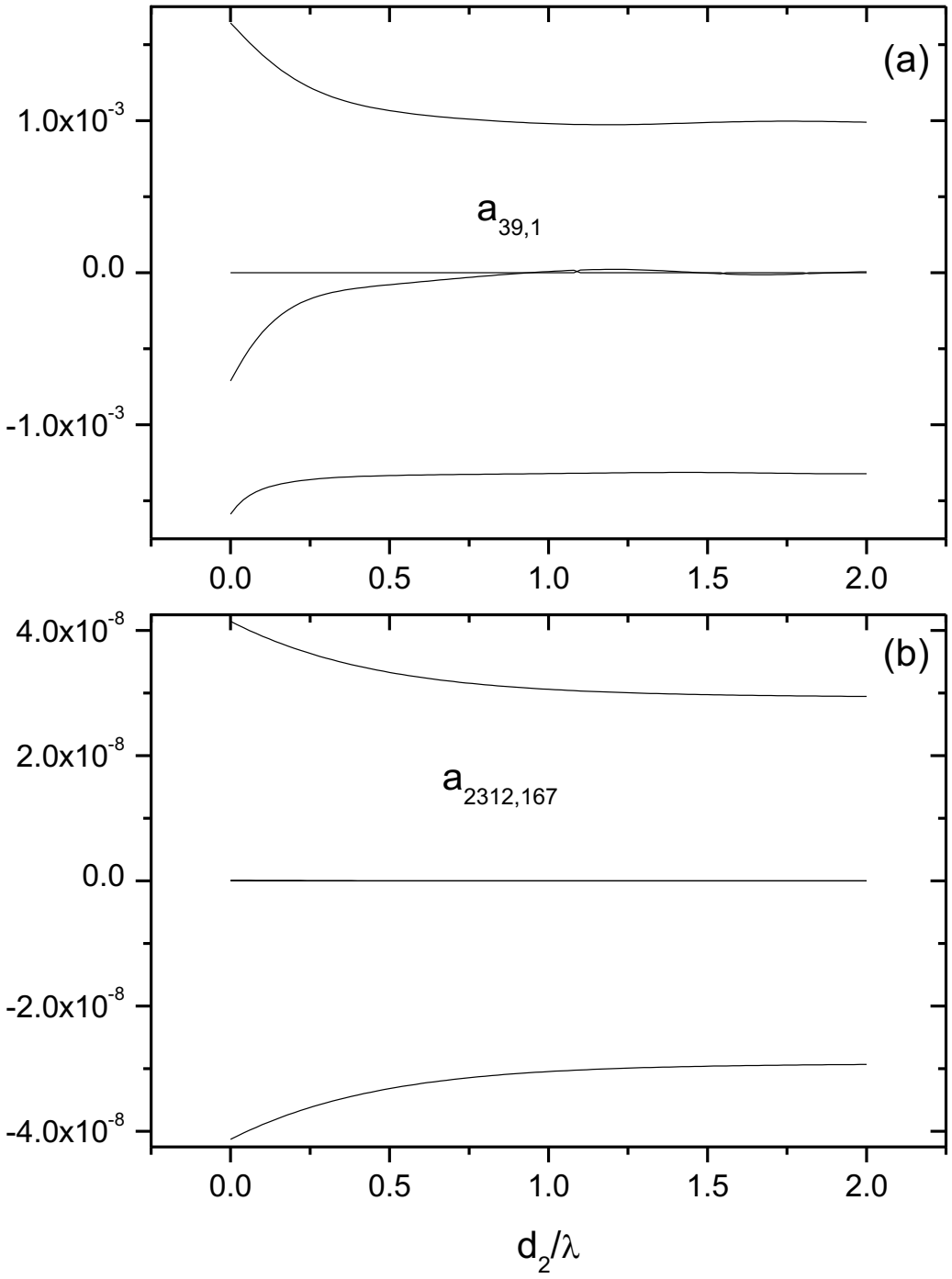


Fig.6 S Dutta Gupta and G S Agarwal, "Quantum optics & …"